Biointerface Research in Applied Chemistry
Open-Access Journal (ISSN: 2069-5837)

Article
Volume 14, Issue 6, 2024, 132

Computational Insights into the Interaction of Muscimol with Human Serum Albumin

Khairul Azreena Bakar [1], Ng Yan Hong [1], Shevin Rizal Feroz [1,2,*]
https://doi.org/10.33263/BRIAC146.132

[1] Department of Biological Sciences and Biotechnology, Faculty of Science and Technology, Universiti Kebangsaan Malaysia, 43600 Bangi, Selangor, Malaysia; p109997@siswa.ukm.edu.my (K.A.B); yhong0407@gmail.com (N.Y.H); shevin@ukm.edu.my (S.R.F);
[2] Structural Biology and Protein Engineering Group, Universiti Kebangsaan Malaysia, 43600 Bangi, Selangor, Malaysia; (S.R.F);
* Correspondence: shevin@ukm.edu.my;

Scopus Author ID 55251086800
Received: 13.03.2024; Accepted: 6.10.2024; Published: 10.12.2024

Abstract: Muscimol (MCM) is a psychoactive compound derived from the *Amanita muscaria* mushroom. It is known for its hallucinogenic properties and is primarily responsible for the psychoactive effects of the mushroom. The interaction of bioactive compounds with plasma transport proteins greatly affects their pharmacological profile and, thus, their potential therapeutic effects. Accordingly, using computational approaches, we investigated the interaction of MCM with the primary carrier protein in humans, human serum albumin (HSA). The preferred binding site of MCM is suggested at site III of HSA (binding energy: –6.56 kcal/mol), with sites I and II acting as less stable possible binding sites. Hydrogen bonds and van der Waals forces primarily contributed to stabilizing the MCM–HSA complexation, with possible involvement of ionic forces. An unfavorable interaction involving Ser-287 was identified as the cause of the reduced stability of MCM docking at site I.

Keywords: muscimol; human serum albumin; drug-protein interaction; molecular docking.

1. Introduction

Muscimol (MCM; 5-aminomethyl-3-isoxazolol), a phytochemical found in the *Amanita muscaria* mushroom (commonly referred to as the fly agaric) [1], holds significant interest in neuroscience research due to its structural similarity (Figure 1) to gamma-aminobutyric acid (GABA) and its potent $GABA_A$ receptor agonist properties [2,3]. As the first proven full agonist of $GABA_A$ receptors, it has led to synthesizing other full agonists, such as nipecotic acid, tiagabine, and gaboxadol [4]. It is well-recognized for its ability to evoke altered perceptions, vivid hallucinations, and sensory shifts, as well as for its sedative and muscle relaxant effects via its GABAergic activity [1,2,5]. Although preclinical studies suggest the potential of MCM in reducing anxiety, its practical application faces hurdles due to concerns related to its toxicity and hallucinogenic properties [6,7].

In general, the interaction between a drug and plasma transport proteins significantly influences the drug's pharmacokinetic and pharmacodynamic properties [8]. The distribution, bioavailability, and duration of the drug's activity within the body are all greatly affected by this interaction [9]. Characterizing the interactions between drugs and plasma transport proteins, especially human serum albumin (HSA), is essential for comprehending and

predicting a drug's pharmacological behavior, including its *in vivo* efficacy, possible adverse effects, and overall therapeutic suitability [10,11].

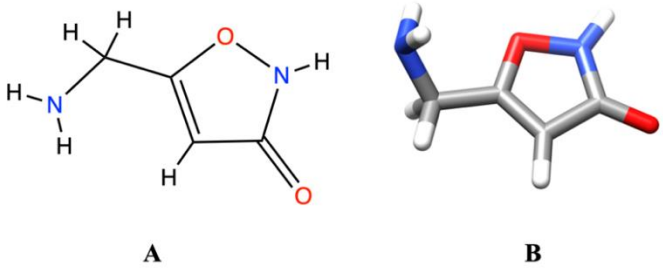

Figure 1. Structure of MCM in **(a)** 2D; **(b)** 3D configurations.

Human serum albumin (HSA) plays a pivotal role as the most abundant and versatile drug-binding protein in the human circulatory system [12]. HSA demonstrates remarkable binding capacity for a diverse range of drugs, with a notable affinity for acidic drugs and, to some extent, neutral and basic ligands [13,14]. There are three distinct binding sites that most drugs tend to bind to on HSA, commonly denoted as sites I, II, and III, which are located in subdomains IIA, IIIA, and IB, respectively [13,15–17]. Additionally, HSA is a negative acute protein and serves as a crucial biomarker in various diseases such as cancer, rheumatoid arthritis, ischemia, obesity, and diabetes [18,19].

Considering its prominent role in drug transport, biomolecular interactions involving HSA are of particular interest in pharmacological studies. Due to the scarcity of available information on the interaction between MCM and HSA, investigating their association through bioinformatics approaches offers valuable insights. In this work, molecular docking, a vital computational tool in drug discovery to predict binding between small molecules and target proteins, was performed to understand the characteristics of the interaction of MCM with HSA. This investigation is instrumental in understanding the potential transport mechanism of MCM in the bloodstream that contributes to its neuropharmacological effects.

2. Materials and Methods

Computational docking analyses were performed to examine the potential binding between MCM and HSA, using Autodock 4.2.6 coupled with AutodockTools 1.5.6 [20]. The HSA conformer (PDB ID: 1BM0) was downloaded from the Protein Data Bank [21], while the MCM structural configuration was retrieved from PubChem (ID: 4266). For docking accuracy, energy minimization with MMFF94 was carried out using Chem 3D version 22.0.0.22. The structure of MCM was represented in the PDBQT format using OpenBabel version 3.1.1 [22]. The existing protein water molecules were eliminated, and any missing atoms were checked and reconstructed. The atomic coordinates of chain A of HSA were extracted and utilized as inputs for AutoDockTools. Subsequently, polar hydrogen atoms, Kollman united partial atom charges, and solvation parameters were incorporated. For MCM, default Gasteiger charges were applied, and nonpolar hydrogens were merged.

For site-specific docking to the three ligand binding sites in subdomains IIA, IIIA, and IB, grids of 70 × 70 × 70 points with a spacing of 0.375 Å were created. These grids were centered at coordinates x = 35.26, y = 32.41, and z = 36.46 for site I (subdomain IIA); x = 14.42, y = 23.55, and z = 23.31 for site II (subdomain IIIA), and x = 42.45, y = 24.47, and z = 15.28 for site III (subdomain IB). Ligand binding energy evaluation was performed using the Lamarckian genetic algorithm with local search (100 runs for each binding site). These

parameters included a population of 150 individuals, 27,000 generations, and 250,000 energy evaluations. The operator weights for crossover, mutation, and elitism were set to 0.8, 0.02, and 1, respectively. Cluster analysis was performed on the docking data using a root-mean-square deviation (RMSD) tolerance of 2.0 Å. The configuration with the most favorable binding energy was visualized and evaluated for post-docking analysis using ADT and UCSF Chimera version 1.17.3 [23]. Biovia Discovery Studio software v21.1.0.20298 (https://www.3ds.com/) was used to predict the intermolecular interactions resulting from the docking contacts.

3. Results and Discussion

3.1. Binding locus.

The cluster analysis of the docking simulations of MCM on HSA at the three main binding sites (after 100 runs) is shown in Figure 2. Based on the binding energy, the docking of MCM at site III was most favorable, with the lowest binding energy of −6.56 kcal/mol. However, this value was slightly less negative than those obtained with the other binding sites, which were −6.43 kcal/mol and −6.33 kcal/mol for sites II and I, respectively. This indicates that while site III is preferred as the binding locus, binding of MCM to the other sites is possible and not thermodynamically unfavorable. The most stable conformation of MCM at each of these three sites is depicted in Figure 3, together with the amino acid residues that are central to the ligand–protein association (details of the interactions are presented in section 3.2).

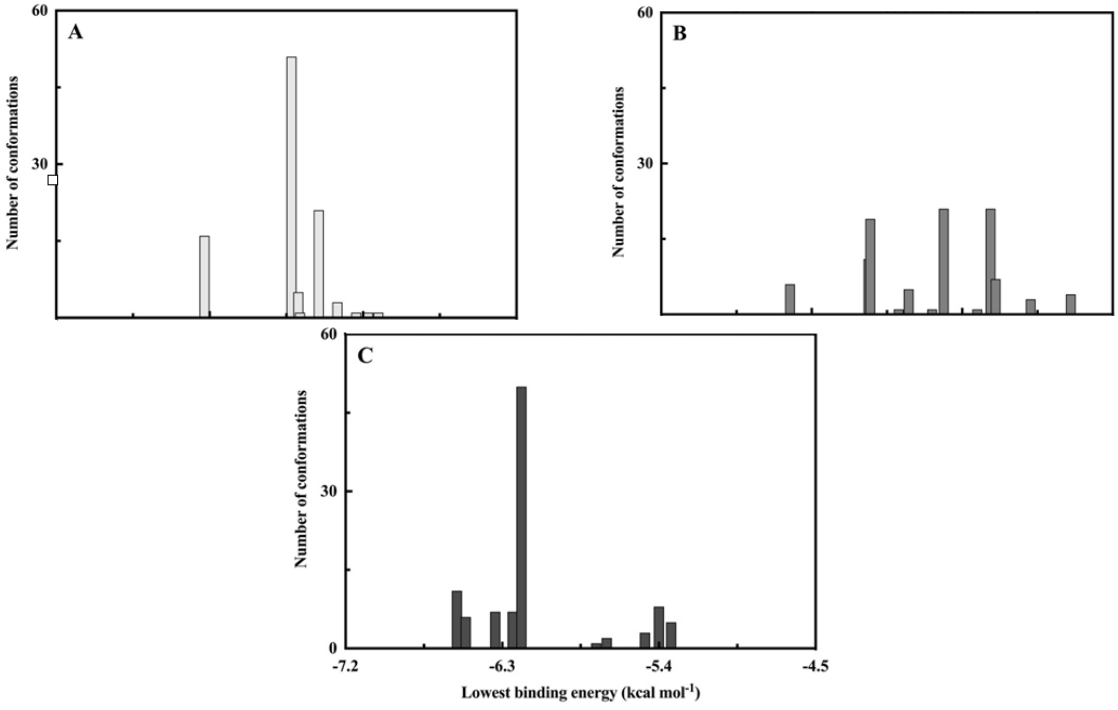

Figure 2. Cluster assessment of site-specific docking of MCM on HSA (PDB ID: 1BM0) with 100 runs for **(a)** site I at subdomain IIA; **(b)** site II at subdomain IIIA; **(c)** site III at subdomain IB.

The possibility of MCM binding to multiple sites on HSA is supported by its fairly small structure, which allows it to easily adapt to different binding pockets with varying structural characteristics. Furthermore, previous studies have elucidated that other GABA receptor agonists also interact with HSA at different sites [24]. For instance, a novel platinum (IV) complex of pregabalin was bound to HSA at subdomain IIA [25], while another GABA

derivative known as methyl 4-(4-((2-(tert-butoxy)-2-oxoethyl)(4-methoxyphenyl)amino)benzamido)butanoate was docked to the domain I of HSA [26]. Collectively, these findings emphasize the intricate binding preferences and interactions exhibited by diverse GABA derivatives towards distinct sites on HSA.

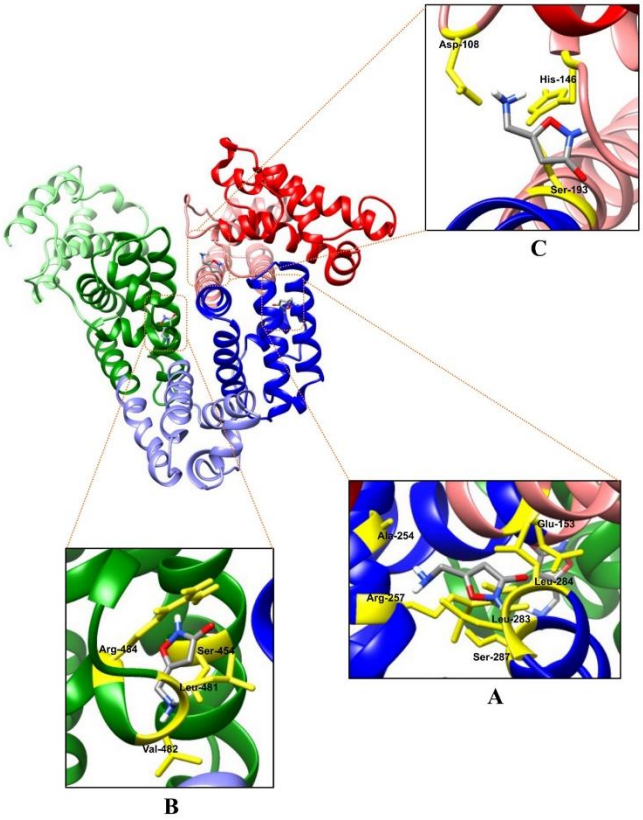

Figure 3. The binding orientations of MCM within binding sites I, II, and III on HSA display the lowest docking energy conformation of MCM after 100 runs. The HSA subdomains are color-coded as follows: red for IA, light red for IB, blue for IIA, light blue for IIB, green for IIIA, and light green for IIIB. The magnified views of the binding sites show the amino acid residues of the protein (illustrated in yellow) interacting with MCM at **(a)** site I in subdomain IIA; **(b)** site II in subdomain IIIA; **(c)** site III in subdomain IB.

3.2. Intermolecular forces.

To gain insight into the types of intermolecular forces involved in the interaction between MCM and HSA, a structural analysis of MCM was conducted using the ChemAxon (*Chemicalize*) program. As depicted in Figure 4, only one microspecies of MCM (microspecies 5) existed with a significant percentage of distribution (93.4%) at the physiological pH of 7.4. The zwitterionic nature of microspecies 5 demonstrates the capability of MCM to undergo ionization under specific conditions, thereby enabling it to partake in ionic interactions with oppositely charged residues of HSA. Additionally, the log*D* value of MCM is predicted to be −2.19 at pH 7.4, suggesting the hydrophilicity of the molecule and the plausible participation of hydrogen bonds in the complexation of MCM with proteins. This is supported by the presence of two hydrogen donors and three hydrogen acceptors in its structure. Furthermore, the topology polar surface area (TPSA) of MCM measures 63.35 Å^2, also suggesting its hydrophilic nature and its suitability for intestinal absorption [27]. Moreover, MCM has a van der Waals volume of 95.08 Å^3 and a van der Waals surface area of 145.94 Å^2. These parameters on the dimension and configuration of MCM shed light on the significance of van der Waals forces and their interactions with neighboring molecules within biological systems.

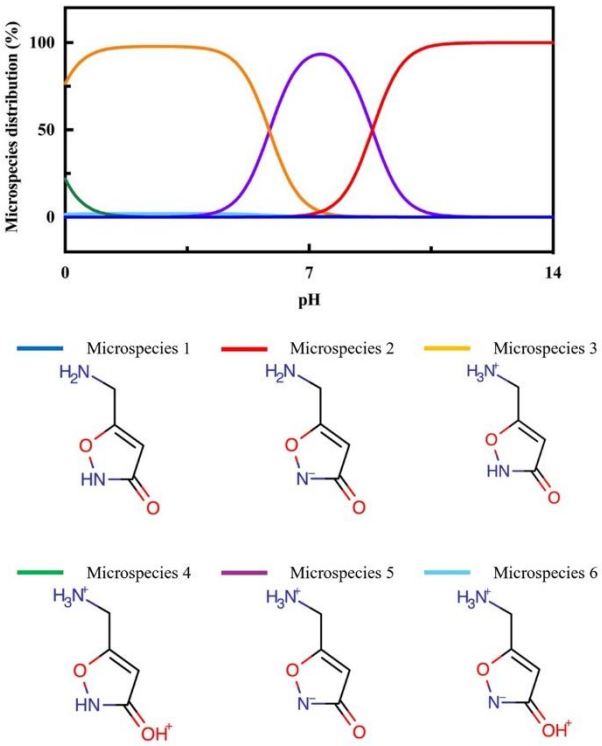

Figure 4. pH-dependent distribution of MCM microspecies.

The docked MCM conformers were also analyzed using Biovia Discovery Studio to obtain more detailed information on the formation of intermolecular interactions with HSA. The intermolecular forces illustrated in Figure 5 (details presented in Table 1) are in line with the type of forces as predicted earlier based on the structural analysis of MCM. The binding of MCM to the three sites is mainly characterized by hydrogen bonds, with multiple bonds (bond lengths ranging from 2.1 to 3.2 Å) formed with the protein's amino acid residues. This is supplemented to a smaller extent by the van der Waals forces, which are relatively weaker than hydrogen bonds. Interestingly, an unfavorable donor-donor interaction involving a nitrogen atom of Ser-287 and a hydrogen atom of MCM was found at site I (Figure 5A), indicating a potential clash between these atoms in the molecular complex. This likely resulted in site I being the least stable docking site for MCM based on binding energy despite forming the most number of hydrogen bonds and van der Waals interactions with the ligand. In summary, the collaborative interplay of hydrogen bonds and van der Waals interactions serves as the fundamental contributor towards the stability of the MCM–HSA complex.

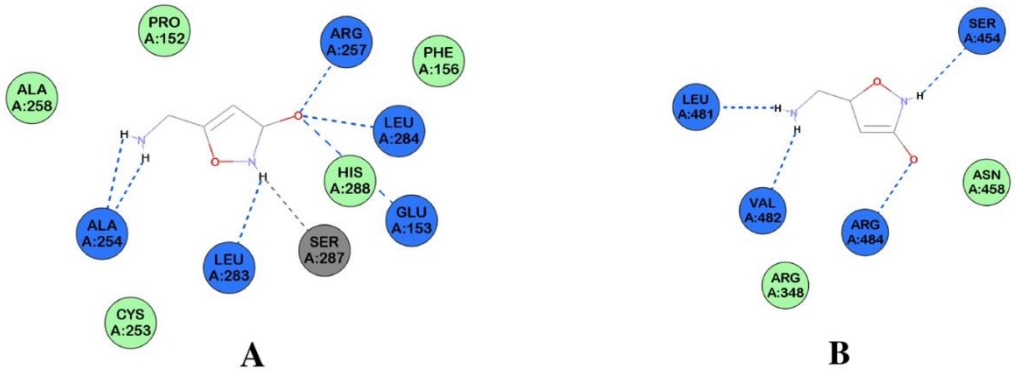

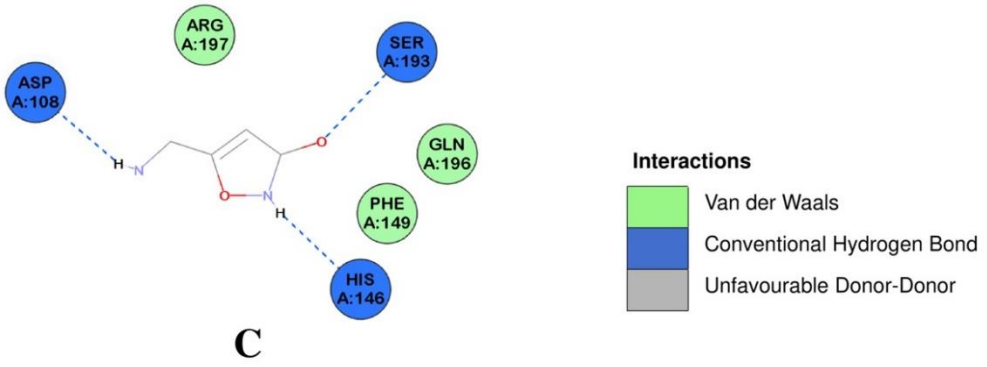

Figure 5. Schematic diagrams revealing the intermolecular forces and amino acid residues involved in the interaction of MCM with subdomains **(a)** IIA, **(b)** IIIA; **(c)** IB of HSA.

Table 1. Details of the intermolecular interactions between MCM and sites I, II, and III of HSA.

Site	Type of interaction	Interaction point	Distance (Å)	Interaction point
I	Conventional hydrogen bond	Leu-283	2.104	MCM: H– Leu-283:O
		Leu-284	2.636	MCM: O– Leu-284:O
		Glu-153	3.259	MCM: O– Glu-153: OE2
		Arg-257	2.168	Arg-257: HH11– MCM:O
		Ala-254	2.167	MCM: H– Ala-254:O
		Ala-254	2.208	MCM: H– Ala-254:O
	Unfavourable donor-donor	Ser-287	2.288	Ser-287: HN– MCM: H
II	Conventional hydrogen bond	Val-482	2.170	MCM: H– Val-482:O
		Leu-481	1.975	MCM: H– Leu-481:O
		Arg-484	2.114	Arg-484: HH12– MCM:O
		Ser-454	2.249	MCM: H– Ser-454:O
III	Conventional hydrogen bond	His-146	2.129	MCM: H– His-146:O
		Ser-193	2.613	MCM: O– Ser-193:O
		Asp-108	2.080	MCM: H– Asp-108: OD1

4. Conclusions

In conclusion, docking simulations revealed that the most thermodynamically favorable binding site for MCM on HSA is at site III. Nevertheless, binding events involving sites I and II are likely as the binding energies recorded for these sites are not markedly dissimilar to those at site III. In general, conventional hydrogen bonds and van der Waals forces collectively contributed towards the stability of the complexation between MCM and HSA at all three main drug binding sites, with the possibility of ionic interactions. However, an unfavorable interaction was observed at site I, resulting in the reduced docking stability of MCM.

Funding

This research was supported by Universiti Kebangsaan Malaysia through the GUP-2021-055 research grant.

Acknowledgments

Declared none.

Conflicts of Interest

The authors declare no conflict of interest.

References

1. Akk, G.; Germann, A.L.; Sugasawa, Y.; Pierce, S.R.; Evers, A.S.; Steinbach, J.H. Enhancement of Muscimol

Binding and Gating by Allosteric Modulators of the $GABA_A$ Receptor: Relating Occupancy to State Functions. *Mol Pharmacol*. **2020**, *98*, 303–313, https://doi.org/10.1124/molpharm.120.000066.
2. Ramawad, H.A.; Paridari, P.; Jabermoradi, S.; Gharin, P.; Toloui, A.; Safari, S.; Yousefifard, M. Muscimol as a treatment for nerve injury-related neuropathic pain: a systematic review and meta-analysis of preclinical studies. *Korean J. Pain* **2023**, *36*, 425–440, https://doi.org/10.3344/kjp.23161.
3. Okhovat, A.; Cruces, W.; Docampo-Palacios, M.L.; Ray, K.P.; Ramirez, G.A. Psychoactive Isoxazoles, Muscimol, and Isoxazole Derivatives from the *Amanita* (Agaricomycetes) Species: Review of New Trends in Synthesis, Dosage, and Biological Properties. *Int. J. Med. Mushrooms* **2023**, *25*, 1–10, https://doi.org/10.1615/IntJMedMushrooms.2023049458.
4. Janković, S.M.; Dješević, M; Janković, S.V. Experimental GABA A Receptor Agonists and Allosteric Modulators for the Treatment of Focal Epilepsy. *J. Exp. Pharmacol*. **2021**, *13*, 235–244, https://doi.org/10.2147/JEP.S242964.
5. Jahanabadi, S.; Amiri, S.; Karkeh-abadi, M.; Razmi, A. Natural psychedelics in the treatment of depression; a review focusing on neurotransmitters. *Fitoterapia* **2023**, *169*, 105620, https://doi.org/10.1016/j.fitote.2023.105620.
6. Moss, M.J.; Hendrickson, R.G. Toxicity of muscimol and ibotenic acid containing mushrooms reported to a regional poison control center from 2002–2016. *Clin. Toxicol*. **2019**, *57*, 99–103, https://doi.org/10.1080/15563650.2018.1497169.
7. Dushkov, A.; Vosáhlová, Z.; Tzintzarov, A.; Kalíková, K.; Křížek, T.; Ugrinova, I. Analysis of the Ibotenic Acid, Muscimol, and Ergosterol Content of an Amanita Muscaria Hydroalcoholic Extract with an Evaluation of Its Cytotoxic Effect against a Panel of Lung Cell Lines In Vitro. *Molecules* **2023**, 28, 6824, https://doi.org/10.3390/molecules28196824.
8. Abubakar, M.; Mohamed, S.B.; Abd Halim, A.A.; Tayyab, S. Use of computational and wet lab techniques to examine the molecular association between a potent hepatitis C virus inhibitor, PSI-6206 and human serum albumin. *Spectrochim Acta - Part A Mol. Biomol. Spectrosc.* **2023**, *294*, 122543, https://doi.org/10.1016/j.saa.2023.122543.
9. Dombi, G.; Horváth, P.; Fiser, B.; Mirzahosseini, A.; Dobó, M.; Szabó, Z.-I.; Tóth, G. Enantioselective Human Serum Albumin Binding of Apremilast: Liquid Chromatographic, Fluorescence and Molecular Docking Study. *Int. J. Mol. Sci*. **2023**, *24*, 2168, https://doi.org/10.3390/ijms24032168.
10. Tayyab, S.; Feroz, S.R. Chapter Nine - Serum albumin: clinical significance of drug binding and development as drug delivery vehicle. In Advances in Protein Chemistry and Structural Biology, Donev, R., Ed.; Academic Press: **2021**; Volume 123, pp. 193-218, https://doi.org/10.1016/bs.apcsb.2020.08.003.
11. Erkmen, C.; Bozal-Palabiyik, B.; Tayyab, H.; Kabir, M.Z.; Mohamad, S.B.; Uslu, B. Exploring molecular interaction of cefpirome with human serum albumin: *In vitro* and *in silico* approaches. *J. Mol. Struct*. **2023**, 1275, 134723, https://doi.org/10.1016/j.molstruc.2022.134723.
12. Ishima, Y.; Maruyama, T.; Otagiri, M.; Chuang, V.T.G.; Ishida, T. The New Delivery Strategy of Albumin Carrier Utilizing the Interaction with Albumin Receptors. *Chem. Pharm. Bull*. **2022**, *70*, 330–333, https://doi.org/10.1248/cpb.c21-01024.
13. Ashraf, S.; Qaiser, H.; Tariq, S.; Khalid, A.; Makeen, H.A.; Alhazmi, H.A.; Ul-Haq, Z. Unraveling the versatility of human serum albumin – A comprehensive review of its biological significance and therapeutic potential. *Curr. Res. Struct. Biol*. **2023**, *6*, 100114, https://doi.org/10.1016/j.crstbi.2023.100114.
14. Peng, M.; Xu, Y.; Wu, Y.; Cai, X.; Zhang, W.; Zheng, L.; Du, E.; Fu, J. Binding Affinity and Mechanism of Six PFAS with Human Serum Albumin: Insights from Multi-Spectroscopy, DFT and Molecular Dynamics Approaches. *Toxics* **2024**, *12*, 43, https://doi.org/10.3390/toxics12010043.
15. Asngari, N.J.M.; Bakar, K.A.; Feroz, S.R.; Razak, F.A.; Halim, A.A.A. Interaction mechanism of a cysteine protease inhibitor, odanacatib, with human serum albumin: *In vitro* and bioinformatics studies. *Biophys. Chem.* **2024**, *305*, 107140, https://doi.org/10.1016/j.bpc.2023.107140.
16. Li, X.; Yan, X.; Yang, D.; Chen, S.; Yuan, H. Probing the Interaction between Isoflucypram Fungicides and Human Serum Albumin: Multiple Spectroscopic and Molecular Modeling Investigations. *Int. J. Mol. Sci*. **2023**, *24*, 12521, https://doi.org/10.3390/ijms241512521.
17. Bteich, M. An overview of albumin and alpha-1-acid glycoprotein main characteristics: highlighting the roles of amino acids in binding kinetics and molecular interactions. *Heliyon* **2019**, *5*, e02879, https://doi.org/10.1016/j.heliyon.2019.e02879.
18. di Masi, A. Human Serum Albumin: From Molecular Aspects to Biotechnological Applications. *Int. J. Mol. Sci*. **2023**, *24*, 4081, https://doi.org/10.3390/ijms24044081.

19. Boesiger, F.; Poggioli, A.; Netzhammer, C.; Bretscher, C.; Kaegi-Braun, N.; Tribolet, P.; Wunderle, C.; Kutz, A.; Lobo, D.N.; Stanga, Z.; Mueller, B.; Schuetz, P. Changes in serum albumin concentrations over 7 days in medical inpatients with and without nutritional support. A secondary post-hoc analysis of a randomized clinical trial. *Eur. J. Clin. Nutr.* **2023**, *77*, 989–997, https://doi.org/10.1038/s41430-023-01303-w.
20. Morris, G.M.; Huey, R.; Lindstrom, W.; Sanner, M.F.; Belew, R.K.; Goodsell, D.S.; Olson, A.J. AutoDock4 and AutoDockTools4: Automated docking with selective receptor flexibility. *J. Comput. Chem.* **2009**, *30*, 2785–2791, https://doi.org/10.1002/jcc.21256.
21. Sugio, S.; Kashima, A.; Mochizuki, S.; Noda, M.; Kobayashi, K. Crystal structure of human serum albumin at 2.5 Å resolution. *Protein Eng. Des. Sel.* **1999**, *12*, 439–446, https://doi.org/10.1093/protein/12.6.439.
22. O'Boyle, N.M.; Banck, M.; James, C.A.; Morley, C.; Vandermeersch, T.; Hutchison, G.R. Open Babel: An open chemical toolbox. *J. Cheminformatics* **2011**, *3*, 33, https://doi.org/10.1186/1758-2946-3-33.
23. Pettersen, E.F.; Goddard, T.D.; Huang, C.C.; Couch, G.S.; Greenblatt, D.M.; Meng, E.C.; Ferrin, T.E. UCSF Chimera—A visualization system for exploratory research and analysis. *J. Comput. Chem.* **2004**, *25*, 1605–1612, https://doi.org/10.1002/jcc.20084.
24. Du, Z.; Chen, H.; Cai, Y.; Zhou, Z. Pharmacological use of gamma-aminobutyric acid derivatives in osteoarthritis pain management: a systematic review. *BMC Rheumatol.* **2022**, *6*, 28, https://doi.org/10.1186/s41927-022-00257-z.
25. Shahabadi, N.; Amiri, S.; Taherpour, A. Human serum albumin binding studies of a new platinum (IV) complex containing the drug pregabalin: experimental and computational methods. *J. Coord. Chem.* **2019**, *72*, 600–618, https://doi.org/10.1080/00958972.2019.1568419.
26. Pal, U.; Pramanik, S.K.; Bhattacharya, B.; Banerji, B.; Maiti, N.C. Binding interaction of a *gamma*-aminobutyric acid derivative with serum albumin: an insight by fluorescence and molecular modeling analysis. *Springerplus* **2016**, *5*, 1121, https://doi.org/10.1186%2Fs40064-016-2752-x.
27. Maximo da Silva, M.; Comin, M.; Santos Duarte, T.; Foglio, M.A.; De Carvalho, J.E.; Do Carmo Vieira, M.; Nazari Formagio, A.S. Synthesis, Antiproliferative Activity and Molecular Properties Predictions of Galloyl Derivatives. *Molecules* **2015**, *20*, 5360–5373, https://doi.org/10.3390/molecules20045360.